

UNCLASSIFIED

## Defense Technical Information Center Compilation Part Notice

ADP010529

TITLE: Design and Aerodynamic Optimization of a  
New Reconnaissance Very Light Aircraft through  
Wind-Tunnel Tests

DISTRIBUTION: Approved for public release, distribution unlimited

This paper is part of the following report:

TITLE: Aerodynamic Design and Optimisation of  
Flight Vehicles in a Concurrent  
Multi-Disciplinary Environment [la Conception et  
l'optimisation aerodynamiques des vehicules  
aeriens dans un environnement pluridisciplinaire  
et simultane]

To order the complete compilation report, use: ADA388284

The component part is provided here to allow users access to individually authored sections of proceedings, annals, symposia, ect. However, the component should be considered within the context of the overall compilation report and not as a stand-alone technical report.

The following component part numbers comprise the compilation report:

ADP010499 thru ADP010530

UNCLASSIFIED

# Design and Aerodynamic Optimization of a New Reconnaissance Very Light Aircraft through Wind-Tunnel Tests

V. Giordano D. P. Coiro F. Nicolosi L. Di Leo

Dipartimento di Progettazione Aeronautica

University of Naples "Federico II"

Via Claudio 21 - 80125 Napoli - Italy

Fax : +39 081 624609 e-mail : [fabrnico@unina.it](mailto:fabrnico@unina.it)

## ABSTRACT

Design of a new Very Light Aircraft (V.L.A.) called G97 *Spotter* has been carried out at DPA (Department of Aeronautical Engineering) and an extensive wind tunnel test campaign has been performed on both aircraft and airfoil models. Wind tunnel tests have guided in the design phase allowing configuration optimization. Effects of nacelle and air intake shape, fuselage stretching, wing incidence and flap/aileron effectiveness have been analyzed through wind tunnel tests.

The airfoil has also been designed and modified with the help of wind tunnel test results obtained for a model.

Optimization of the airfoil leading edge shape has been done and has brought to a sensible drag reduction at high speed conditions. Optimization of the air intake shape on the aircraft model has been performed leading to a configuration characterized by lower drag. Influence of an air intake fairing has been analyzed and tested through wind tunnel tests. Wing stall path has been studied.

Importance of wind tunnel tests as a device to analyze and design light aircraft configuration has been highlighted.

## INTRODUCTION

Primary applications of G97 *Spotter* V.L.A. are observation/reconnaissance, offering helicopter-like view from cockpit and good low-speed handling and loiter capabilities. The fuselage shape has been designed in order to achieve these goals with a large transparent nose section with two wide transparent doors. The airplane is characterized by an high cantilever wing and is powered by rear pushing propeller engine.

The aircraft schematic views are shown in fig. 1.

Due to the unusual configuration an extensive wind tunnel test campaign has been performed on a 1:5.7 scale model (fig. 2, 3) to obtain aircraft aerodynamic characteristics.

Wind tunnel tests will be presented in this paper as a fundamental tool to carry on a good design, even for very light and ultra-light aircraft.

The performances of light aircraft in commerce are really close between them and only through an accurate design of aircraft components and through an accurate configuration study a new aircraft can be really competitive. When unusual configurations (like that one studied in the present paper) are designed, wind tunnel tests becomes essential to understand the aerodynamic behavior, to estimate the importance of each of aircraft components (i.e. for the drag breakdown) and to help in the design of particular part like engine nacelle, air intake and aircraft tail which can be easily modified on the model and tested in the design phase.

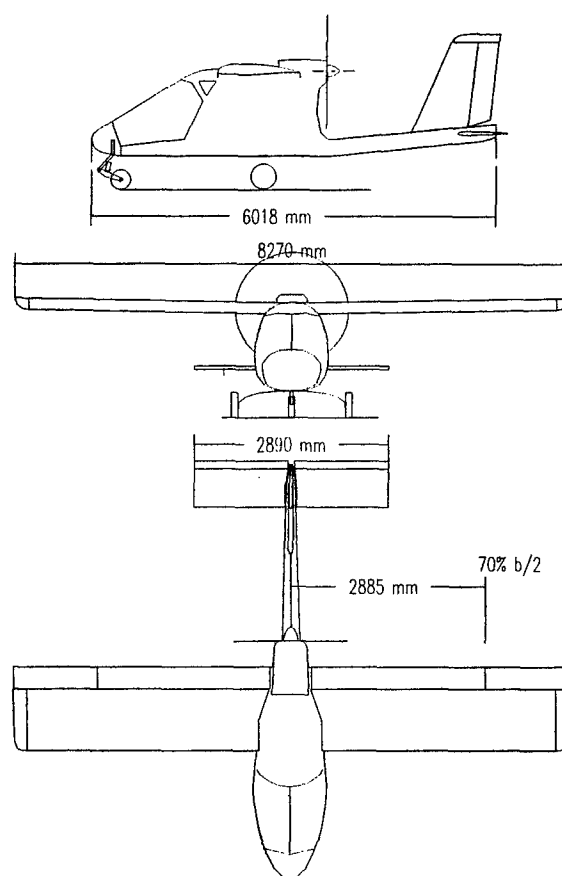


Fig. 1: G97 aircraft schematic views

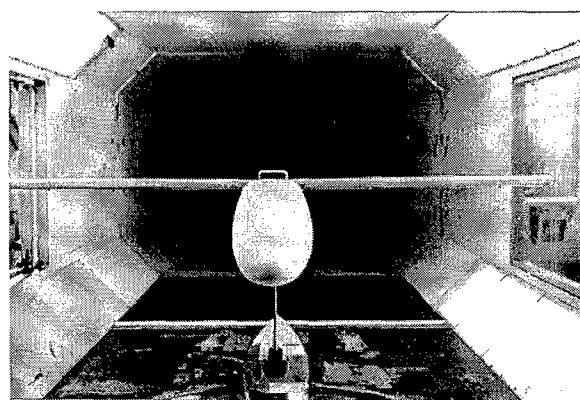


Fig. 2 : G97 model in DPA WT test section

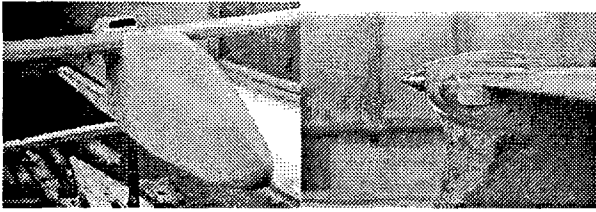


Fig. 3 : G97 model - Lateral view  
Particular of Engine Nacelle

For G97 aircraft the airfoil design has been a fundamental step for the whole configuration. The high lift airfoil, called VG1-13 (13% thickness) and specifically designed for this aircraft, has been extensively tested in DPA wind tunnel.

Numerical investigations have also been performed on this airfoil and some of numerical codes developed in the past at DPA have been used to estimate airfoil aerodynamic characteristics and to guide the designer in modifying the model tested in the tunnel. Through wind tunnel tests performed on the airfoil model has been possible to verify if the l.e. modification were in accord with numerical prediction. Primary goals of leading edge modification was the reduction of drag through the improvement of lower surface flow.

In the past other light aircraft like P92 and P96 have been extensively tested [1] at DPA in the wind tunnel and optimized configurations have been the result of the test campaign. In example the leading edge fairing of P96 low-wing aircraft has been designed through wind tunnel tests that have shown reduced separation at wing root.

Wind tunnel tests, paying carefully attention to Reynolds number effects, can lead to an estimation of aircraft performances which can be compared to data coming from numerical evaluations (panel code [ref. 2] , semi-empirical methods[ref. 3]) or comparison with similar aircraft with the same engine.

Flight tests can give indications on some possible improvements in the aircraft aerodynamics which can be verified through wind tunnel tests before implementing the final modification on the aircraft.

## TEST SETUP

Wind tunnel tests on the aircraft model and on the 2D airfoil model (see fig. 4) have been performed in the DPA wind tunnel which is a closed circuit low speed tunnel with a test section of 2 m. wide and 1.4 m. height.

The maximum Reynolds number is about 3 million per meter and the turbulence level is about .1% at the test section center. Tests on the airfoil have been performed by pressure measurements on a 2D model with 0.75 m. chord spanning the test section and a wake rake has been used to estimate airfoil drag. Tests on the aircraft model have been performed using a strain gage based three-component balance to measure lift, moment and drag.

## AIRFOIL TESTS

An aluminum model with 0.75 m chord spanning vertically the test section (see fig. 4) has been tested. The airfoil shape is shown in fig. 5.

The airfoil characterized by forward and rearward camber, is 13.4 % thick and has been designed to have good high lift capabilities.

The original airfoil showed very high drag characteristics at high speed conditions and it was then modified at the leading edge (fig. 6) to improve flow conditions on the lower surface. The original airfoil showed at negative angles of attack (cruise conditions) an high negative pressure peak which leads to flow separation on forward part of lower surface.

Airfoil optimization has been performed through numerical codes developed at DPA and a new leading edge shape has been designed. The airfoil model has been modified and tested again.

Lift curves relative to the original and to the modified airfoil (called VG1-13H) are shown in fig. 7. The airfoil maximum lift coefficient at  $Re=1.8$  mil. is about 1.60 and the airfoil can be then considered like a high lift airfoil. The leading edge modification does not lead to any considerable lift decrease.

Due to strong blockage effect at high angles of attack (the airfoil chord over test section width ratio is 0.4) the airfoil stall has been measured on a new model with 0.45 m chord.

In fig. 8 the experimental lift curve at  $Re=1.1$  mil. of the smaller model compared to that one relative to the 0.75 m chord model at the same Reynolds number is shown. The airfoil maximum lift coefficient has been measured to be 1.62 and different post-stall behavior respect to the bigger model can be observed. At  $Re=1.8$  mil. (flight conditions at stall) the airfoil maximum lift coefficient is expected to be between 1.65 and 1.70.

Airfoil drag polar at  $Re=1.8$  mil. of original and modified airfoil are shown in fig. 9. The original airfoil was characterized by a high negative pressure peak on the lower surface at low and negative angles of attack.

In fig. 10 pressure distributions on original and modified airfoils at low angle of attack are shown. The graph put in evidence the different flow conditions on airfoil lower surface which leads to lower drag. The original airfoil at  $\alpha=-4$  deg. is characterized by a separated flow region on lower surface, while the modified airfoil shows a high negative pressure peak with completely attached flow. The airfoil was then characterized by small separated area on lower surface with consequent drag increase at high speed cruise conditions. In fact the original airfoil has very high drag at lift coefficients lower than  $0.30 \div 0.40$ . The modified airfoil shows improved behavior at low lift coefficient, being characterized by acceptable drag also at high speed cruise conditions ( $C_l$  around 0.20).

Drag coefficient at high speed conditions have then been reduced and brought to acceptable values.

In fig. 11 airfoil moment coefficient (respect to 0.25 c) at  $Re=1.8$  mil. are shown. The airfoil is characterized by quite high moment coefficient (around -.10) which is a penalty regarding tail trim drag and torsional loads at high speed. The airfoil on the aircraft will be mounted with the rear part deflected 5 deg. upward to reduce moment coefficient.

The airfoil is currently under a refinement phase through both numerical and experimental investigations.

Numerical versus experimental data comparison has been presented in [4].

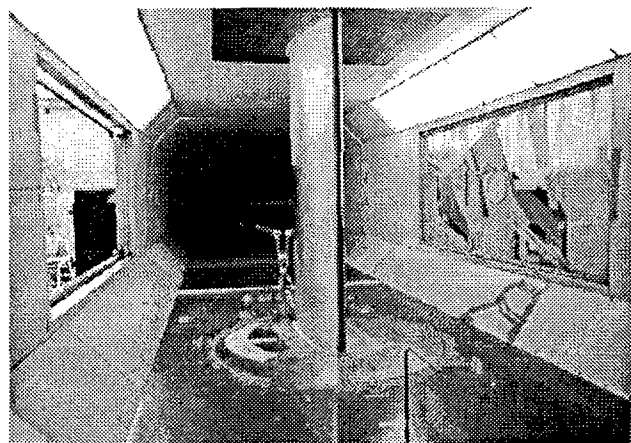


Fig. 4 : Airfoil model in DPA wind tunnel test section

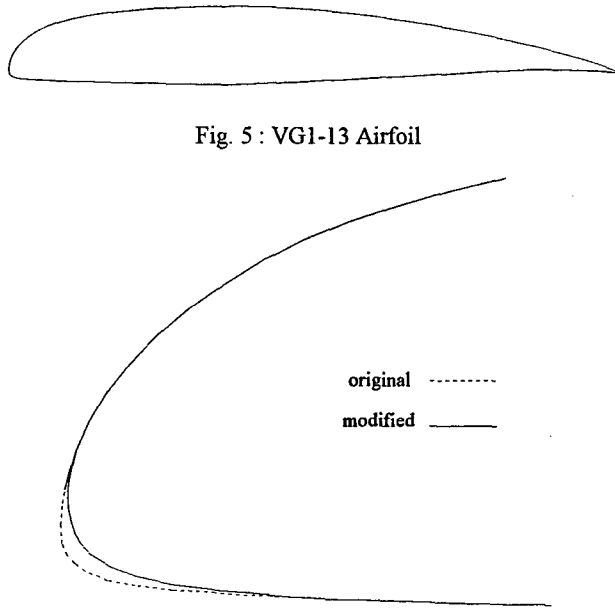


Fig. 5 : VG1-13 Airfoil

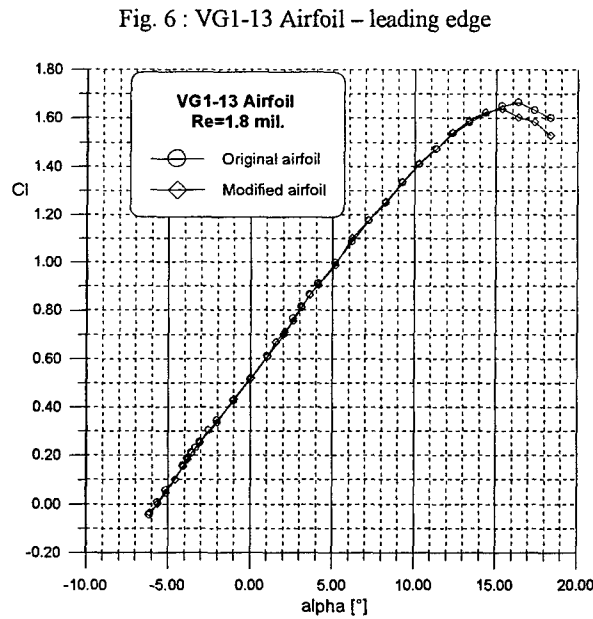


Fig. 6 : VG1-13 Airfoil - leading edge

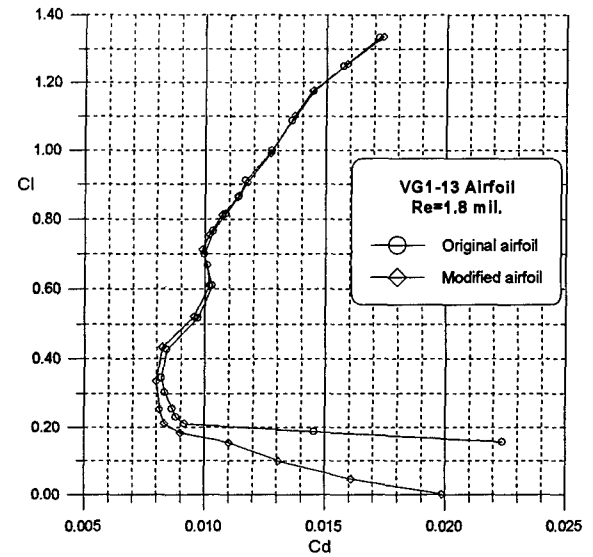


Fig. 9 : VG1-13 Airfoil - drag polar

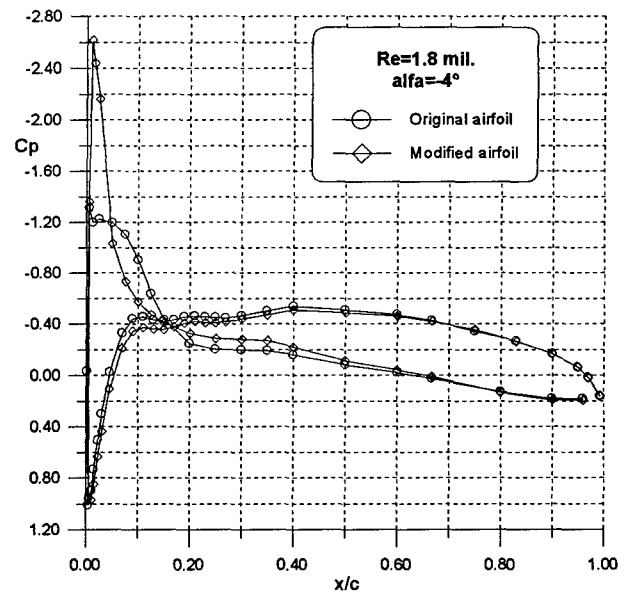


Fig. 10 : VG1-13 Airfoil - press. coeff. distribution

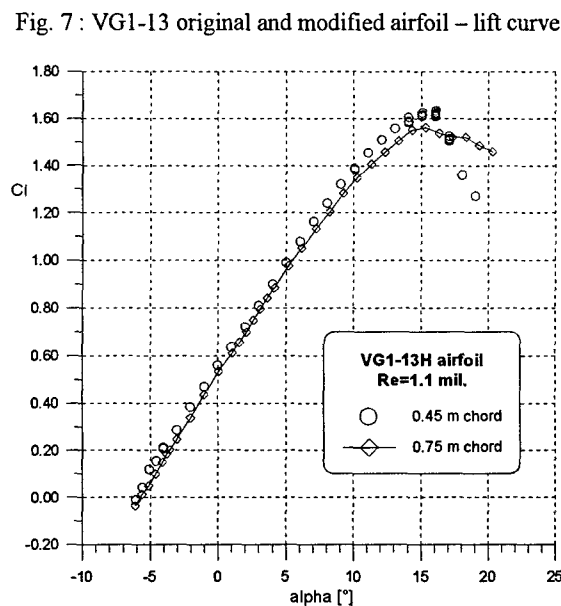


Fig. 8 : VG1-13H airfoil - lift curve of 2 models

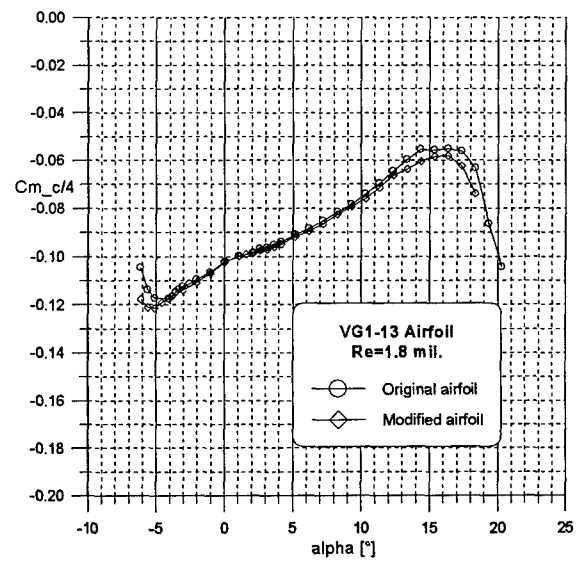


Fig. 11 : VG1-13 Airfoil - moment coeff. curves

AIRCRAFT MODEL TESTS

Configuration aerodynamic analysis and optimization has been performed through wind tunnel tests on the aircraft model.

Wind tunnel tests have been performed on a 1:5 scale wood model of G97 wing-body. The model has been built reproducing the exact configuration, including the real engine nacelle and air intake shape. Pictures showing the wing-body model mounted in DPA wind tunnel test section are shown in fig. 2 and 3. In fig. 3 the lateral view shows the fuselage shape and the engine nacelle reproduction in scale.

Different flap/aileron configurations

The wing on the model has been built in such a way to allow various settings of flap/aileron deflections. The goal was to test also the configuration obtained deflecting the flap and aileron 5° upward obtaining a reduced moment coefficient suitable for high-speed cruise. The model airfoil geometry with trailing edge movable part deflected 5° upward and set at 0° is shown in fig. 12. The wing with flap and aileron top view is shown in fig. 13. Other tested configurations obtained deflecting flap/aileron are shown in table 1.

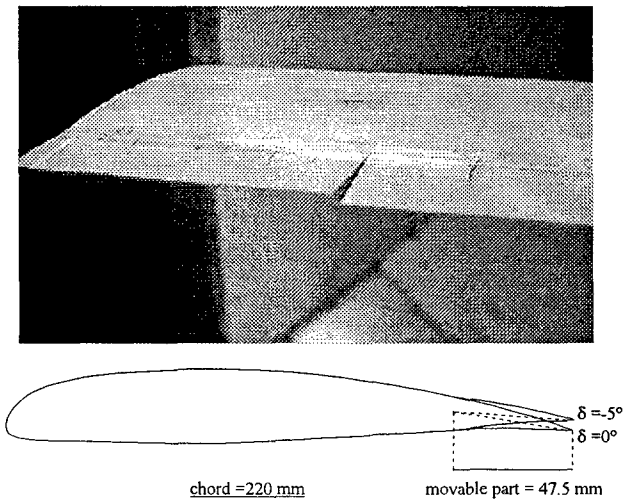


Fig. 12 : wing model flap/aileron

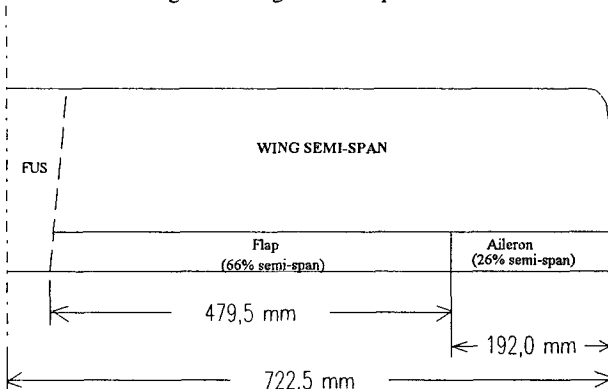


Fig. 13 : Wing semi-span model top view

CONF.	Flap	Aileron
A (High speed)	$\delta=-5^\circ$	$\delta=-5^\circ$
B (Low speed)	$\delta=0^\circ$	$\delta=-5^\circ$
C	$\delta=0^\circ$	$\delta=0^\circ$

Table 1 : Wing flap/aileron configurations

The test Reynolds number referred to the wing chord ( $c=0.22$  m) is about 0.6 mil. The difference of Reynolds number between wind-tunnel tests and flight has to be taken carefully in account comparing aerodynamic coefficients obtained for both airfoil models and flight. Wind tunnel tests for flap/aileron configuration A,B,C have been performed. Configuration A (with flap and aileron deflected -5° upward) is thought to be the final aircraft configuration for high speed. At lower speed, with flap set at 0°, conf. B is the other operative configuration. The upward deflection has been foreseen to reduce the moment coefficient which is too high for VG1-13H airfoil. Configuration C is not an operative condition for the real aircraft, but it is useful to check aileron effectiveness.

In fig. 14 the lift coefficient curves versus alpha for the 3 different configurations is shown. The maximum lift coefficient for configuration A is reduced form 1.45 (conf. C) to 1.35. Wing-body lift coefficients are in good agreement with scaled (to 3D effects) two-dimensional values measured on the airfoil model. The flap and aileron effectiveness have been evaluated.

The flap effectiveness  $\tau=(d\alpha/d\delta)$  is :  $\tau=(1.75^\circ/5^\circ)=0.35$

The aileron effectiveness is :  $\tau=(0.95^\circ/5^\circ)=0.19$

The moment coefficient curves for the 3 different configurations, evaluated respect to the estimated real aircraft C.G. position ( $X_{c.g.} = 23.3\%$  chord and  $Z_{c.g.} = 29.3\%$  chord under wing level) are shown in fig. 15. The moment coefficient at  $\alpha=0^\circ$  with flap and aileron deflected 5° upward (conf. A) is reduced from -0.12 (relative to conf. C) to -0.08. This value seems reasonable to limit wing torsional load and tail equilibrium load at high speed. The moment coefficient versus CL curve shows a static stability for CL greater than 0.6, typical of high-wing configurations. The slope in the linear range indicates a position of the wing-body aerodynamic center of about 19% of the chord.

In fig. 16 the drag polars for conf. A,B,C are shown. Conf. A is characterized by a drag coefficient of 0.028 while conf. C has a considerable increase of drag at low lift coefficient with a value around 0.035. The advantage of adopting conf. A at high speed instead of conf. B is also underlined by this favorable effect. The drag increase of conf. C at low lift coefficients is mainly due to the airfoil which is working at negative angles of attack and is characterized by areas of separated flow on lower surface (like in fig. 11). The polar curve for conf. A is parabolic for CL between 0.20 and 1.00 and is characterized by a  $C_{Do}=0.025$  and an Oswald efficiency factor of 0.72.

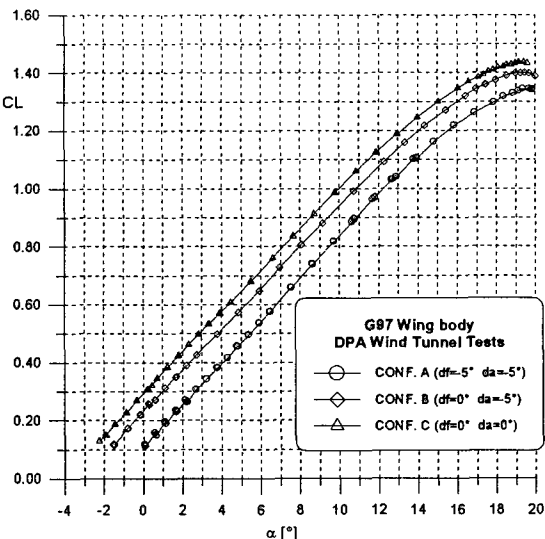


Fig. 14 : Wing-body Lift curves for different flap/aileron configurations

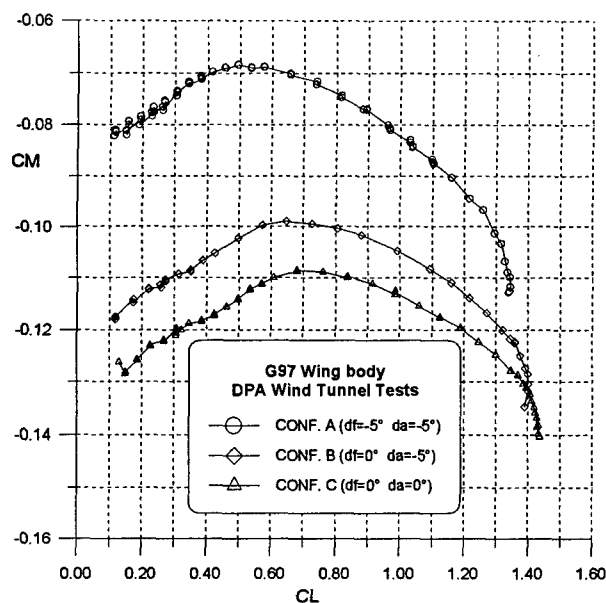


Fig. 15 : Wing-body moment curves for different flap/aileron configurations

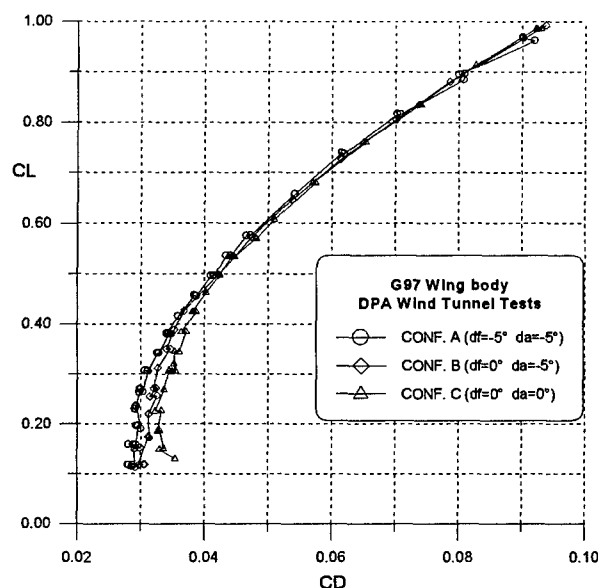


Fig. 16 : Wing-body drag polars for different flap/aileron configurations

#### Effect of engine nacelle and air intake

Effect of engine nacelle and air intake has been investigated. Two different nacelles with different air intake frontal area have been tested. Tests have been performed also with a fin instead of the nacelle and the air intake to estimate their contribution to the total drag.

Pictures of lateral views of nacelle N1, N2 and fin are shown in fig. 17.

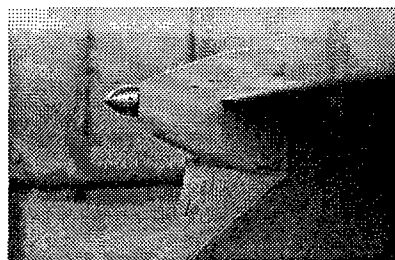
In fig. 18 is clearly noticeable the difference in air intake frontal area between nacelle N1 and N2. The intake of nacelle N1 was modified to reduce frontal area and flow separation on the top and shape N2 was chosen.

With nacelle N2 (smaller than the first one) a 25% drag reduction has been obtained as shown in the wing-body drag polar relative to wing configuration A (fig.19).

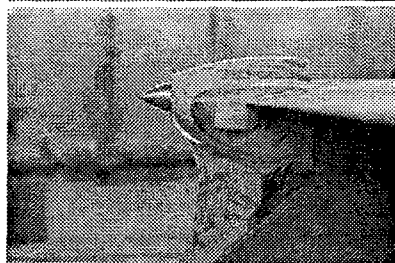
In the same figure the drag polar relative to the configuration with fin is shown. It can be seen that configuration N2 leads to drag values not so higher than those relative to the configuration with fin. The influence of air intake frontal area is not so critical for configuration N2, however the most

critical aspect which contributes to the high drag increase for configuration N2 appears to be the flow separation on air intake upper surface. In fig. 20 flow visualization with tufts on configuration N1 and N2 at  $\alpha=1^\circ$  are shown. It is clearly visible that conf. N1 presents separated flow (which leads to the higher drag in fig. 19) while conf. N2 is characterized by attached flow conditions.

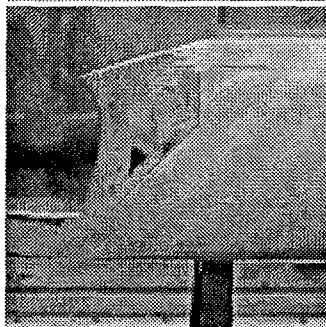
Preliminary flight tests on the aircraft prototype have shown that the second nacelle with smaller air intake does not lead to any danger of insufficient engine cooling.



NACELLE N1



NACELLE N2



FIN

Fig. 17 : Nacelle N1, N2 and fin

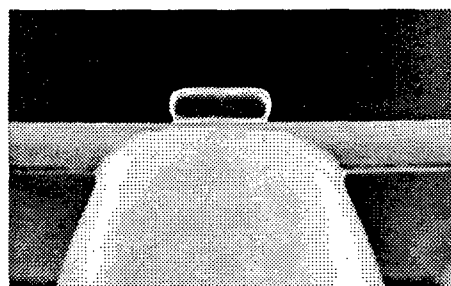
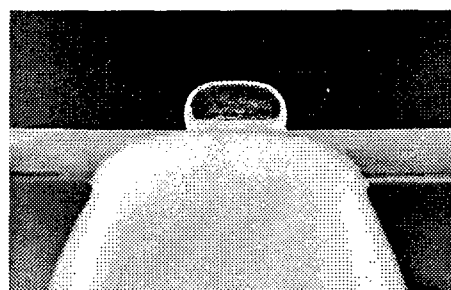


Fig. 18 : Nacelle N1, N2 – frontal view

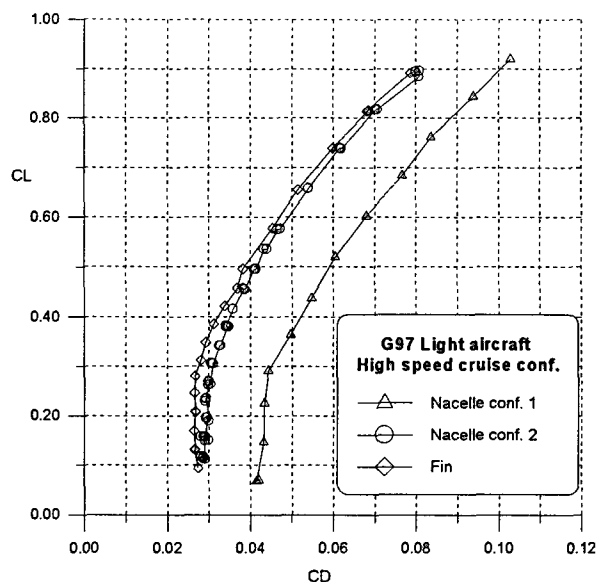
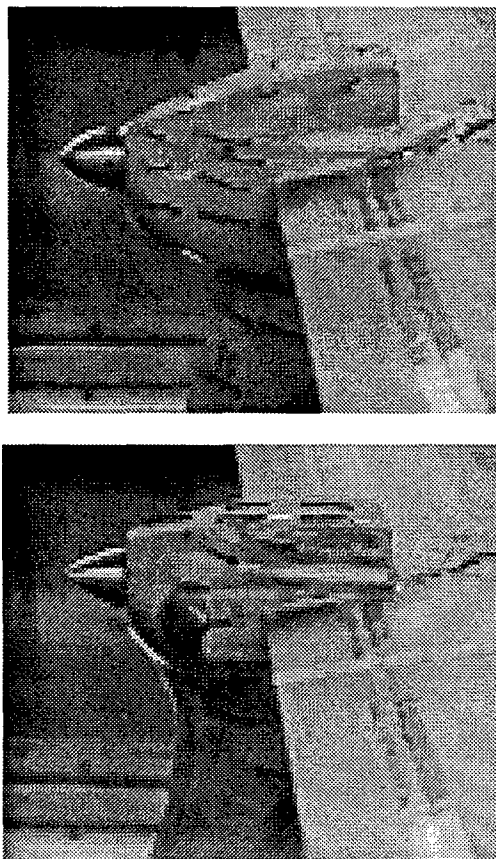


Fig. 19 : Drag Polar, Nacelle N1,N2 and fin

Fig. 20 : Flow visualization on nacelle N1 and N2  
 $\alpha=1$  deg.

### Wing-fuselage junction fairing

The experimental results presented in figg. 14, 15, 16, 19 were obtained with a fairing at both wing fuselage junction and air intake. Wing-fuselage interference effects have been pointed out through panel method calculations [4]. These effects together with more complicated and unpredictable 3D viscous interference effects lead to a drag increase which can be reduced through the use of a proper fairing. More than one fairing shape has been tested and a final very small fairing has been found which leads to a considerable drag reduction.

In fig. 21 the picture shows the fairing at the junction. In fig. 22 drag polars relative to the wing-body configuration A (and nacelle N2) with fairing (also shown in fig. 16 and 19) and without fairing are shown.

It is possible to notice that the fairing is particularly effective at low angles of attack. In fact the fuselage without fairing induces high negative angles of attack at wing root but with the fairing this effect is diminished. This is a desirable effect in view of the fact that the VG1-13H airfoil is characterized by separations and high drag values in this range of angles of attack (fig. 9).

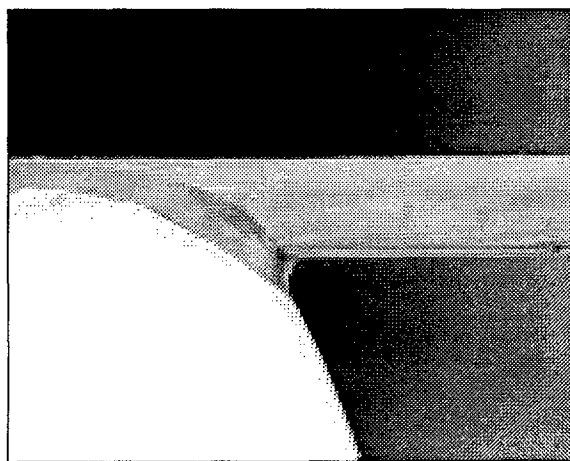


Fig. 21 : Wing-fuselage junction fairing

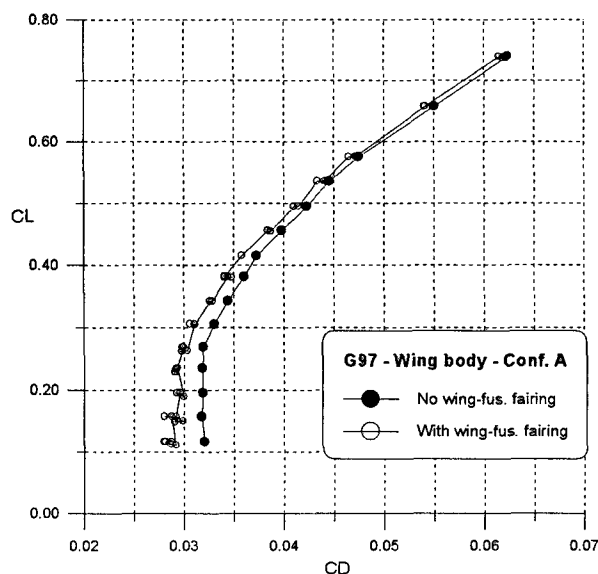


Fig. 22 : Effect on drag of wing-fuselage junction fairing

### Air intake fairing

Effect of a small air intake fairing has been tested. From flow visualization with tufts it appeared that separated flow conditions were present on air intake sides.

To improve and streamline the air intake an air intake fairing has been thought and applied to the model. The air intake is represented in fig. 23 and 24.

Drag polar of configuration A with nacelle N2 and with air intake fairing and without air intake fairing are shown in fig. 25. The use of the air intake fairing leads to a further drag coefficient reduction of almost 10%.

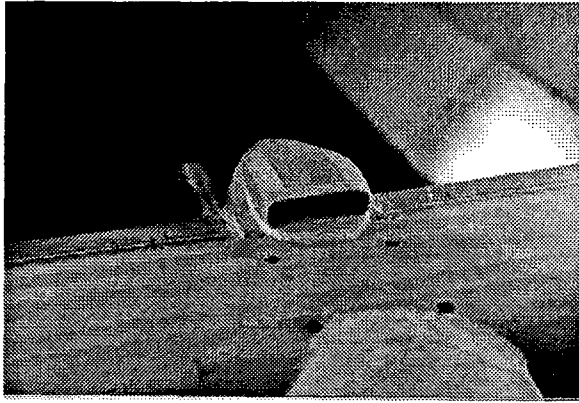


Fig. 23 : Air intake fairing

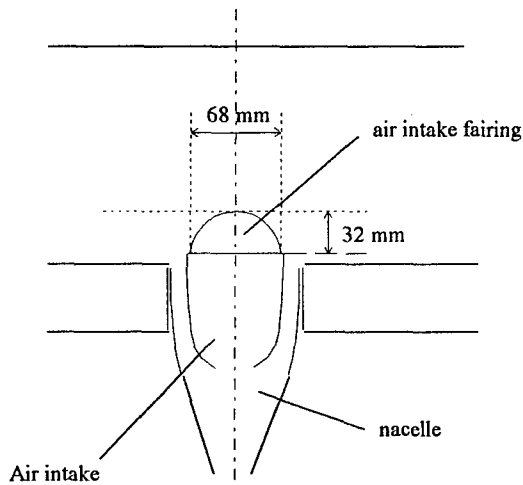


Fig. 24 : Air intake fairing

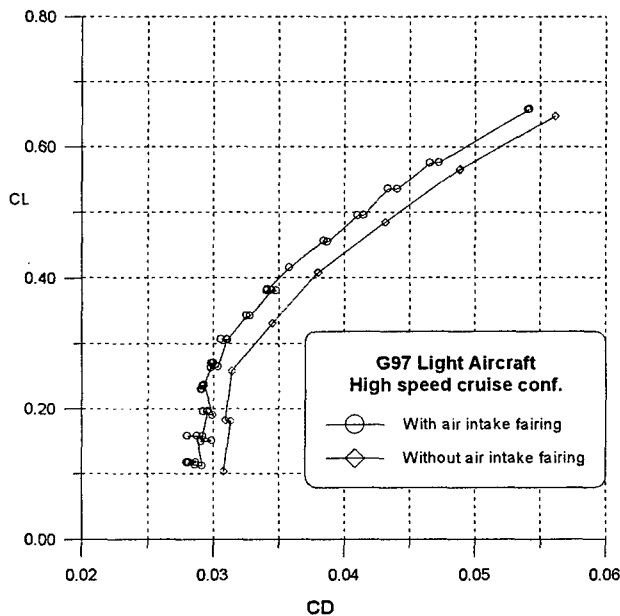


Fig. 25 : Air intake fairing effect on drag

### Fuselage length increase

To shift the C.G. position toward the aircraft nose (it is well known that the rear pushing propeller configuration is critical because the engine weight leads to balance problems) it has been necessary to increase the fuselage length. Effect of fuselage length increase has been tested.

In fig. 26 the lateral view of both original and stretched fuselages is presented.

The fuselage length has been increased of 5 cm on the model (corresponding to about 25 cm for the full scale aircraft).

The effect of length increase (and also of wetted area) on fuselage drag is shown in fig. 27. In this figure the drag coefficient versus angle of attack of the original and stretched fuselage with nacelle is shown. The length increase leads to an average drag coefficient increase of 1+2 counts (about 10% of fuselage drag). It can be seen that the fuselage drag decreases with incidence due to the air intake which becomes less exposed.

The effect of length increase on wing-body moment coefficient (evaluated respect to the aircraft CG position,  $X_{cg}=23.3\%c$  -  $Z_{cg}$  on middle of fuselage height) is shown in fig. 28. It can be noticed that in the linear range (CL between 0 and 0.5) the stretched fuselage is characterized by an increased instability respect to the original one. The aerodynamic center of the wing-body configuration is at 19% of the chord with the original fuselage and at 18% for the stretched fuselage. The moment coefficient (also due to the different wing-fuselage interference effects) is reduced of about 0.01 and this is favorable for equilibrium loads.

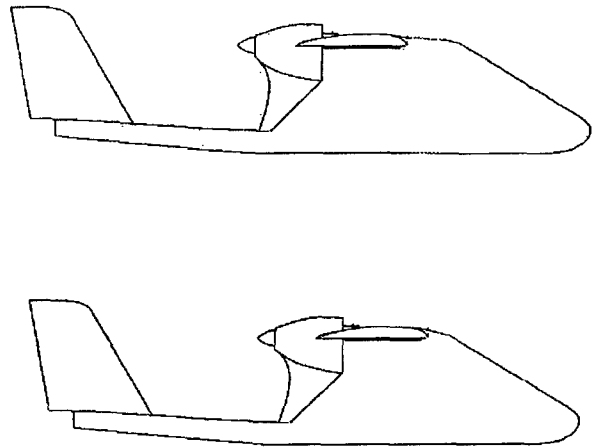


Fig. 26 Original and stretched(on the top) fuselage

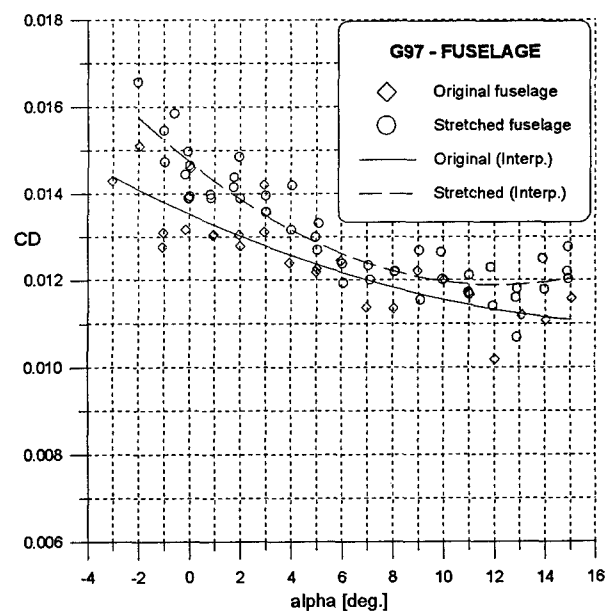


Fig. 27 Fuselage Drag coefficient

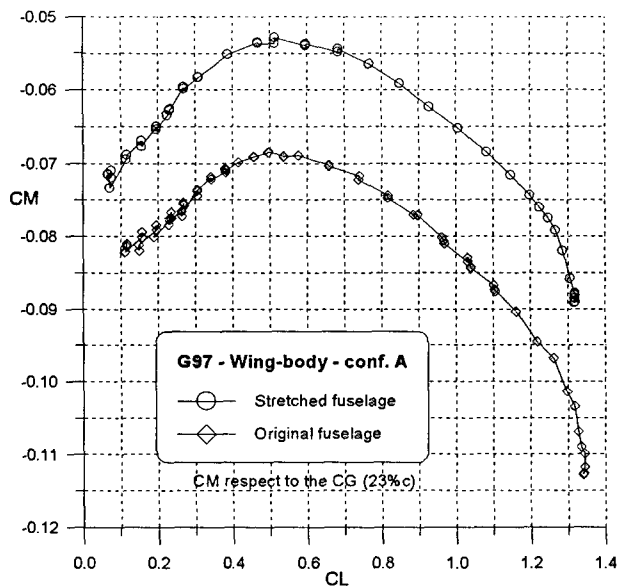


Fig. 28 : Wing-body moment coefficient

### Wing stall path

Investigation on the wing stall path has been performed by visualization with tufts.

Visualizations indicate a stall path similar to a tapered wing due to the effect of the air intake in the middle of the wing.

In fig. 29 flow visualization on wing upper surface at  $\alpha=17^\circ$  deg. is shown. The separated flow region is evidenced in fig. 30. It is clear that the air intake and the nacelle in the center of the wing influences the wing stall and reduces separations at wing root. The aileron region is unaffected by flow separation.

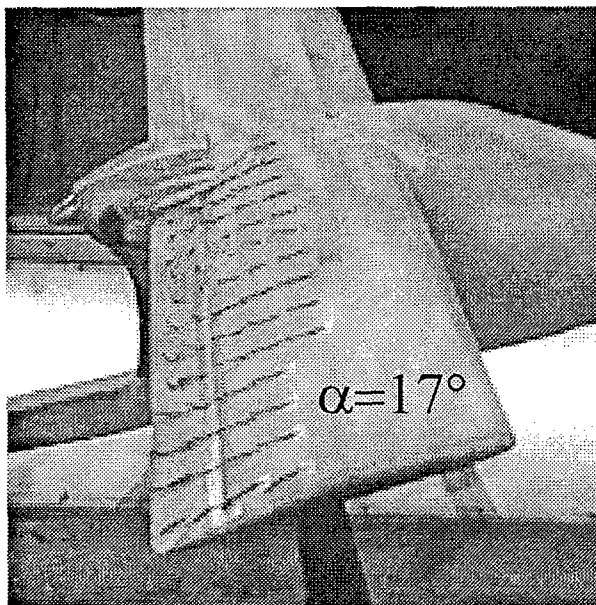
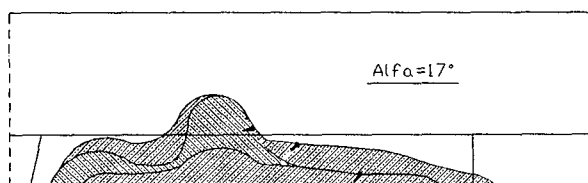
Fig. 29 : Flow visualization,  $\alpha=17^\circ$  deg.

Fig. 30 : Separated region

### Conclusions

Wind tunnel tests have been performed in the low speed wind tunnel belonging to D.P.A. on airfoil and aircraft models of G97 *Spotter* light aircraft.

The airfoil leading edge shape has been optimized leading to a reduced drag coefficient at high speed cruise conditions.

The aircraft model has been tested in several flap/aileron configurations giving indications on flap/aileron effectiveness and a necessary moment coefficient reduction has been obtained deflecting the flap 5 deg. upward.

An accurate analysis has been performed on nacelle and air intake shape. Two different nacelles with different air intake frontal area have been tested. It has been obtained a relevant drag coefficient reduction through a well streamlined nacelle shape. Effect of an air intake fairing has been tested. The fairing leads approximately to a 10% drag reduction on wing-body configuration.

Effect of fuselage length increase has been tested. The "stretched" fuselage leads to a very small drag increase and modifies the moment coefficient and the aerodynamic center of wing-body configuration.

The wing stall path has been analyzed through flow visualization with tufts on wing upper surface.

The air intake at wing center leads to a reduced load and reduced separation at wing root.

Further investigations through wind tunnel tests have been planned in the next future.

Flight tests will give further indications of accuracy of wind tunnel aerodynamic analysis and optimization of this light aircraft.

### References

- [1] Coiro D.P., Marulo F., Nicolosi F., Ricci F.: "Numerical, Wind Tunnel and Flight Tests for P92J and P96 Light Aircraft" XXI I.C.A.S. Congress, Melbourne, AUSTRALIA, Sept. 1998.
- [2] F. Nicolosi, D.P. Coiro : "Fuselage Design and wing integration for Sailplanes and Light Aircraft", XIV AIDAA Congress, Naples October 1997
- [3] Wolowicz, H. C. and Yancey, B. R., " Longitudinal Aerodynamic Characteristics of Light, Twin-Engine, Propeller-Driven Airplanes," NASA TN D-6800, 1972
- [4] Giordano V., Coiro D.P., Nicolosi F., : "Reconnaissance Very Light Aircraft Design. Wind-Tunnel and Numerical Investigation". EHAE 99 Conference, Prague, Sept. 1999. To be published on Journal for theoretical and applied mechanics - Czech Republic.